

New crystal growth process in order to produce YBaCuO superconducting bar sample.

D. GROSSIN*, C. HARNOIS, S. MARINEL and J.G. NOUDEM.

CRISMAT Laboratory 6, Bd Marechal Juin14050 CAEN cedex FRANCE

* Corresponding author: david.grossin@ismra.fr

Abstract: Many processes were utilized in order to produce $\text{YBa}_2\text{Cu}_3\text{O}_{7-\delta}$ (YBCO) bar samples, but up to now, the alignment of single domains with the bar axis was not optimized for power applications. A new process was elaborated to synthesise samples with optimized alignment: the Microwave Top Seeding Floating Zone (MTSFZ). The CeO_2 and SnO_2 doping YBCO composition was selected for its high superconducting properties. Samples of good quality were produced by MTSFZ in very short time thanks to a seed that initiated successfully the correct alignment. The superconducting properties evaluated by SQUID measurements were similar to the ones obtained with other texturing process: critical temperature near to 91 K and critical current density at 77 K in self field of $42 \text{ kA}\cdot\text{cm}^{-2}$.

1. Introduction

Many applications using the superconductor (HTSC) materials have been realized: magnetic applications such as levitation (flywheel) [1,2] and transport applications (current transport and fault current limiter). In our case we focus our investigation on the material prepared for resistive superconducting fault current limiters [3,4] (resistive FCL). This application requests: a high superconductor transport current property and a bar or meander shape. Microwave Floating Zone (MFZ) process [5] is used to produce YBCO textured bar, but the bar length is limited and the orientation of the single domain compare to the sample shape is not optimal. In order to overcome this disagreement, a new microwave process was developed: translation of the sample is horizontal and a seed is used like in the Top Seeding Melt Texture Growth process (TSMTG) [6,7] to control the crystal orientation in contrast to our previous work where the translation was vertical. The combination of seeds and floating zone method was already envisaged by Lee [8] P. Fox [9] and S.Marinel [10]. P.Fox et al. used a horizontal Bridgman furnace with a Sm123 seed on the top of the sample and the authors concluded that in the mix of seeding and floating zone the stability of orientation along a bar was

not satisfying. Indeed, during their process many nucleated new grains appeared and hindered the growth of the seed induced domain. Lee et al. and Marinel et al. used vertical configuration with the seed inside the bar. They showed that the sympathetic nucleation using Sm123 seed was successfully realized but this preferential alignment was generally conserved only along a short distance (1 cm). In our case, we study the effect of the seeding technique combined to the microwave floating zone method in a horizontal furnace with a very high thermal gradient generated by microwave heating. This very high thermal gradient allows increasing the crystal growth rates [11]. The target was to obtain a sample where the initial growth was produced from the seed and where the crystal orientation kept the original alignment. The results obtained are discussed in this paper.

2 Experimental procedures

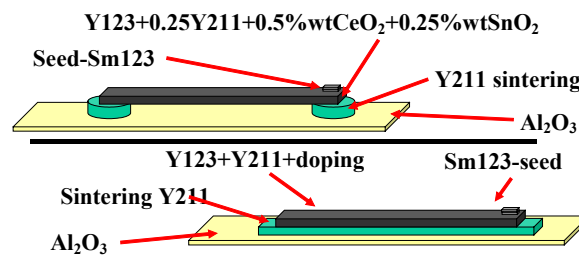


Figure 1: Schematic diagram showing the configuration and two steps in the Microwave Top Seeding Floating Zone, MTSFZ-process (a) self supporting Y123 bar, (b) sample on Y211 substrate.

The powder, Y123 (SR30), Y211 (SSC) 0.25% mol in excess and doping compounds 0.5wt% CeO_2 and 0.25wt% SnO_2 were ground by ball milling in an agate mortar. This powder mixture was isostatically pressed at 300 MPa with latex tube. This bar was placed on a sintered Y211 support in order to limit the loss of liquid phases and the alumina pollution (such as on figure 1). The whole system was placed on long bar alumina enabling a horizontal translation at very low speed (2 mm/h) into a gradient furnace. The heating was obtained through a microwave process: a microwave generator (2.45 GHz sairem GMP20KSM) delivers a variable power from 0 to 2000 W. Rectangular waveguide (WR340) allows the transport of microwave to the tuner and next to the cavity. TE10p Symmetrical resonant cavity [12] transmits the microwave energy to the suscepter. Optimal transfert of the energy to the cavity was obtained thanks to by the tuner (impedance agreement accord) and the

regulation of the length between the coupling iris and the short circuit piston (iris and piston delimit the cavity). The susceptor [12] tube was positioned on the centre of the cavity perpendicular to the electric field. This susceptor absorbs the microwave (by inductive interaction) and the heating was transmitted to the sample by Infra-Red radiation. Into the susceptor tube, no microwave was observed and the thermal gradient (maximum 300°C/cm) as well as the maximal temperature varied according to microwave incident power. In our case, the susceptor material is LaCrO₃, and maximal temperature imposed in this experiment was 1060°C with thermal gradient of $G \approx 180^\circ\text{C}/\text{cm}$.

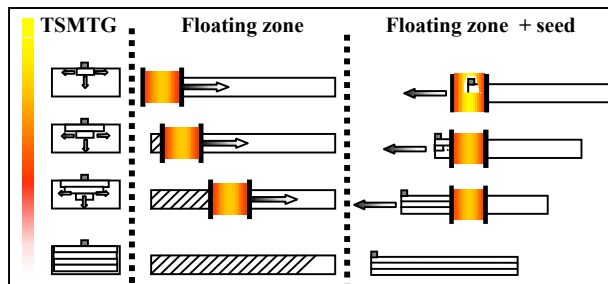


Figure 2: Illustration of the growth mechanism for various process (a) TSMTG, (b) floating zone (FZ) and (c) combination of FZ and seed crystal.

The figure 2 shows the different mechanisms between TSMTG [13], FZ [14], and the Combination of seeding and MFZ-process. In order to confirm or infirm mix mechanisms growth, many samples were made with these conditions, Sm123 seed, translation rate 2mm/h, and the microwave power of 350 W ($G \approx 180^\circ\text{C}/\text{cm}$, $T_{\text{max}} \approx 1070^\circ\text{C}$) : (S_1) with sintered Y211 plots support and the other (10 samples) with sintered Y211 bar support. In order to compare, bars were also made first by the floating zone method without Sm123 seed (S_0) and secondly by TSMTG process (S_{TSMTG}) with thermal cycle described in [15]. Note that in the case of microwave heating, the whole thermal cycle lasted 15 hours for the 3 cm length sample when the chosen TSMTG cycle lasted 90 hours. All bars were annealing in oxygen during 150 hours [16].

Three methods were used to analyse the texture quality: (i) optical microscopy observation (ii) scanning electronic microscopy (SEM) image and (iii) Pole figure with X-Ray diffraction. We can observe the alignment of ab-planes in SEM and optical image owing to the “cracks” and “micro-cracks” that are parallel to ab-planes. Each sample was polished and observed with polarized light through Olympus BH2-HLSH. Philips XL 30 FEG Scanning Electronic

Microscope (SEM) was coupled to back scattered electron (BSE) (oxford instruments) and energy dispersive spectra (EDS) analyser (oxford instruments) in order to characterize microstructure and composition.

The critical temperature (T_c) was measured by SQUID magnetometer (quantum design MPMS 5) on cleaved samples, the applied field being 20 Oe parallel to c axis. The critical current density (J_c) at 77 K was obtained by two methods, (i) SQUID measurements, magnetic field, B was applied perpendicular to cleaved ab-planes (B//c), the data being analysed with the modified Bean model [17] and (ii) D.C. transport measurements at 77K in self field by the four-probe technique with an electric field criterion of $1 \mu\text{V}\cdot\text{cm}^{-1}$.

3 Results and discussion

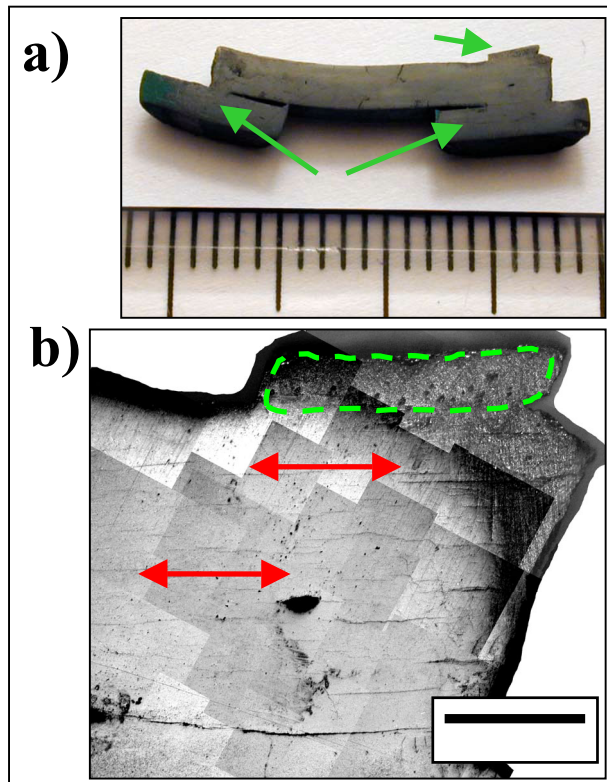


Figure 3: Optical images of the sample S1 showing (a) the cross section of the self supporting Y123 and (b) microstructure with the aligned ab-planes.

The samples namely S1 bar is illustrated on figure 3. This figure points out that the (S1) bar shapes was not preserved during the synthesis. The two Y211 supports induce a mechanical problem: a camber of Y123 samples during this thermal cycle. This result led us to change the support for the next samples: one sintered Y211 bar was successfully used instead of several plots to suppress the camber effect here underlined.

Concerning S0 samples, no preferential crystal orientation has been observed on 3 cm length samples, which present a polycrystalline microstructure. On the contrary one unique grain was initiated from the seed on S1 or S_{TSMTG} samples. The size of this grain can reach the whole bar length in the case of S1 samples (3 cm) but is each time limited to approximately 1 cm in the case of S_{TSMTG} samples, although the cooling rate was adjusted to texture at least 2 cm side domains. This behaviour is assumed to be due to the bar shape. Nevertheless, this point underlines the great advantage of the microwave process that leads to longer textured bars in quite shorter times.

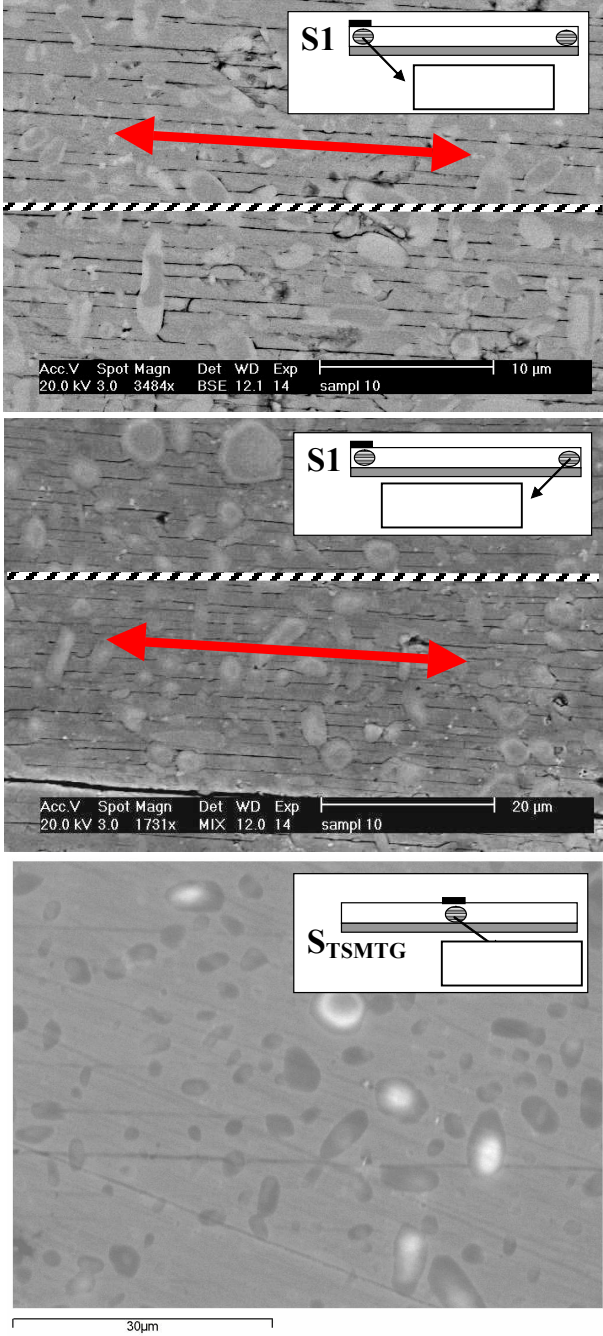


Figure 4: SEM images of the polished zones corresponding to the diagram showing S1 and S_{TSMTG} samples.

S0 samples being polycrystalline their microstructure was not studied. Figure 4 illustrates the microstructures observed in S1 and $S_{TSM TG}$ samples. First of all, figures 6a and 6b correspond respectively to the microstructure under the seed, and at this end of the bar for S1 sample. The alignment of the (ab) planes was the same on two pictures. The same horizontal orientation was observed in all pictures along the bar axis. This shows that the seed induced grain growth has proceeded through the whole bar length.

In both cases microstructure observation reveals dense samples (figure 4c). Sub micrometric Ce and Sn containing particles were found to be homogeneously distributed as it was already noticed in the typical microstructure corresponding to this composition [18]. Several differences can be observed between S_1 and $S_{TSM TG}$: first of all, samples S1 contain more numerous Y211 inclusions. Indeed, since the crystal growth rates are quite larger in the case of S1 samples, more Y211 particles are trapped and can be finally found in the textured material.

Secondly, a large number of ab-planes micro-cracks exist in S1 sample. These cracks are mainly attributed to the very fast cooling of this process which can be approximated $G.R \approx 30^\circ C.h^{-1}$.

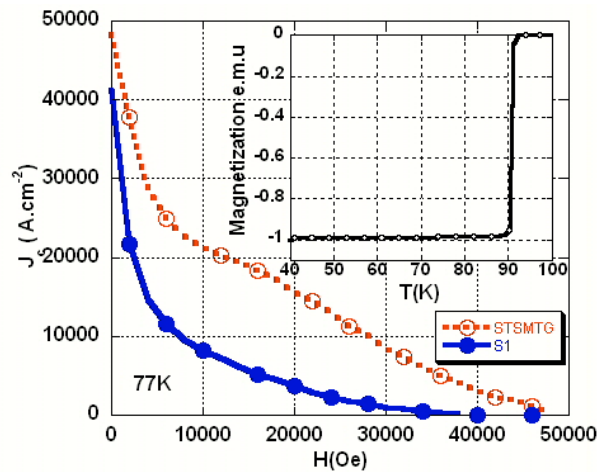


Figure 5: Magnetic field dependence of critical current densities at 77 K for S1 and $S_{TSM TG}$ samples. (Inset) magnetization versus temperature $M(T)$ showing a narrow superconducting transition with a T_c^{onset} of 92 K and a $\Delta T_c = 1.5 K$.

The critical temperature (T_C) and the bean critical current density at 77 K (J_C) are illustrated on figure 5. For both samples, the T_C onset is close to 92 K and the transition width is 1.5 K. The J_C in self field attain 40 to 50 $kA \cdot cm^{-2}$. It appears that the orders of magnitude of the J_C of the two samples are similar. These results are consistent with the values generally obtained with

the same doping samples made by TSMTG [15] and MFZ [19] process. The transport critical current density measured at 77 K was near $5000\text{A}\cdot\text{cm}^{-2}$ when a hot spot located at the contacts for current supply stopped the measurement, hence the real J_C may be better than this result.

4 Conclusion

This article demonstrates that it's possible to ensure the growth of well aligned grain initiated from a seed with Microwave Top Seeding Floating Zone process (MTSFZ). This new process permits to obtain a single domain bar sample with ab-planes parallel to the bar axis and good superconducting properties. The main advantage of this technique is the production of textured samples in very short time. Further investigations are now in progress to increase both the length of the textured bar and the superconducting properties.

References:

- [1] Vajda I, Porjesz T, Györe A, Szalay A, Gawalek W, Conference M²S, February 2000, Houston (USA), Physica C **341-348** (2000) 2609
- [2] Borneman H J, J. Appl. Supercon. **2** (1994) 147
- [3] Tixador P, Buzon D, Floch E, Porcar L, Isfort D, Chaud X, Tournier R, Bourgault D, Barbut J M, Bach J, Physica C **378-381** (2002) 815-822
- [4] Obradors X, Puig T, Granados X, Sandiumenge F, Physica C **378-381** (2002) 1
- [5] Marinel S, Provost J and Desgardin G, Physica C (1998) **294** 129
- [6] Leblond-Harnois C, Monot I and Desgardin G, Physica C (2000) **340** 299
- [7] Nagaya, ISTEC J. **10** (1997) 31
- [8] Lee D F, Partsinevelos C S, Presswood R G and Salama K, Physica C **311** (1994) 211
- [9] Fox P, Hardman E, Tatlock G J and McCartney D G Supercond. Sci. Technol. **9** (1996) 1092
- [10] Marinel S, Bourgault D, Belmont O, Sotelo A, Desgardin G and Raveau B, Inst. Phys. Conf. Ser. No **167**, (2000) IOP Publishing Ltd 159-162
- [11] Cima M. J, Flemings M. C, Figueredo M. A, Nakade M, Ishii H., Brody H. D, Haggerty J.S, J. Appl. Phys. **72** (1992) 179
- [12] Marinel S and Desgardin G Adv. Mater. **10** (1998) 1448

- [13] Morita M, Takebayashi S, Tanaka M, Kimura K, Myamoto K, Sawano K, Adv. Supercond. **3** (1991) 733
- [14] Nakamura Y, Furuya K, Izumi T and Shiohara Y, J.Mater. Res. (1994) **9** 420
- [15] Leblond-Harnois C, Monot-Laffez I and Desgardin G, Physica C **340** (2000) 299
- [16] Leblond C, Monot I, Bourgault D and Desgardin G Supercond. Sci. Technol. **12** (1999) 405
- [17] Bean C.P., Rev. Mod. Phys. **36** (1964) 31
- [18] Harnois C, Hervieu M, Monot-Laffez I and Desgardin G, J. Europ. Ceram. Soc. **21** (2001) 1909
- [19] Marinel S, Monot I and Desgardin G. Supercond. Sci. Technol. **11** (1998) 563